ORIGINAL RESEARCH ARTICLE

Strain imaging to predict response to cardiac resynchronization therapy: a systematic comparison of strain parameters using multiple imaging techniques

Alwin Zweerink[1][*][†], Wouter M. van Everdingen[2][†], Robin Nijveldt[1,8], Odette A.E. Salden[2], Mathias Meine[2], Alexander H. Maass[3], Kevin Vernooy[4,8], Frederik J. de Lange[5], Marc A. Vos[6], Pierre Croisille[7], Patrick Clarysse[7], Bastiaan Geelhoed[3], Michiel Rienstra[3], Isabelle C. van Gelder[3], Albert C. van Rossum[1], Maarten J. Cramer[2][†] and Cornelis P. Allaart[1][†]

[1]*Department of Cardiology, and Amsterdam Cardiovascular Sciences (ACS), VU University Medical Center, Amsterdam, The Netherlands;* [2]*Department of Cardiology, University Medical Center Utrecht, Utrecht, The Netherlands;* [3]*Department of Cardiology, Thorax Centre, University of Groningen, University Medical Center Groningen, Groningen, The Netherlands;* [4]*Department of Cardiology, Maastricht University Medical Center, Maastricht, The Netherlands;* [5]*Department of Cardiology, Academic Medical Center, Amsterdam, The Netherlands;* [6]*Department of Medical Physiology, University of Utrecht, Utrecht, The Netherlands;* [7]*Univ Lyon, UJM-Saint-Etienne, INSA, CNRS UMR 5520, INSERM U1206, CREATIS, F-42023, Saint-Etienne, France;* [8]*Department of Cardiology, Radboud University Medical Center, Nijmegen, The Netherlands*

Abstract

Aims   Various strain parameters and multiple imaging techniques are presently available including cardiovascular magnetic resonance (CMR) tagging (CMR-TAG), CMR feature tracking (CMR-FT), and speckle tracking echocardiography (STE). This study aims to compare predictive performance of different strain parameters and evaluate results per imaging technique to predict cardiac resynchronization therapy (CRT) response.

Methods and results   Twenty-seven patients were prospectively enrolled and underwent CMR and echocardiographic examination before CRT implantation. Strain analysis was performed in circumferential (CMR-TAG, CMR-FT, and STE-circ) and longitudinal (STE-long) orientations. Regional strain values, parameters of dyssynchrony, and discoordination were calculated. After 12 months, CRT response was measured by the echocardiographic change in left ventricular (LV) end-systolic volume (LVESV). Twenty-six patients completed follow-up; mean LVESV change was −29 ± 27% with 17 (65%) patients showing ≥15% LVESV reduction. Measures of dyssynchrony ($SD\text{-}TTP_{LV}$) and discoordination (ISF_{LV}) were strongly related to CRT response when using CMR-TAG (R^2 0.61 and R^2 0.57, respectively), but showed poor correlations for CMR-FT and STE (all $R^2 \leq 0.32$). In contrast, the end-systolic septal strain (ESS_{sep}) parameter showed a consistent high correlation with LVESV change for all techniques (CMR-TAG R^2 0.60; CMR-FT R^2 0.50; STE-circ R^2 0.43; and STE-long R^2 0.43). After adjustment for QRS duration and QRS morphology, ESS_{sep} remained an independent predictor of response per technique.

Conclusions   End-systolic septal strain was the only parameter with a consistent good relation to reverse remodelling after CRT, irrespective of assessment technique. In clinical practice, this measure can be obtained by any available strain imaging technique and provides predictive value on top of current guideline criteria.

Introduction

Guideline recommendations for cardiac resynchronization therapy (CRT) primarily depend on QRS duration and left bundle branch block (LBBB) morphology, resulting in approximately one-third of patients becoming 'non-responders'.[1–3] Despite substantial efforts to improve patient selection for CRT, parameters that better predict CRT response are

currently lacking. Myocardial strain imaging is a promising tool that quantifies the mechanical consequences of LBBB. In-homogeneity of contraction during LBBB reduces left ventricular (LV) pump function efficiency,[4] and CRT subsequently improves LV pump function by restoring mechanical efficiency of the heart.[5,6] Therefore, a variety of strain parameters have been proposed to serve as markers for CRT response over the past years.[7–9] Most of these parameters were introduced using a single-imaging modality, but at present, multiple imaging modalities are available. Cardiovascular magnetic resonance (CMR) imaging offers assessment of myocardial strains using feature tracking (CMR-FT) software on standard cine images,[10–12] or by the implementation of myocardial taglines (CMR-TAG).[8,13–15] Although CMR-TAG is often used as reference technique in scientific research, availability is limited in clinical practice. Speckle tracking echocardiography (STE), on the other hand, is widely available as a bedside tool. Although STE analysis is highly dependent on the quality of the available acoustic windows, this technique also demonstrated predictive value for CRT outcome.[7,9,16] Despite promising results of multiple strain parameters used in single-modality studies, a direct comparison of parameters between available modalities is lacking. Relative differences in strengths and weaknesses between techniques may cause optimal strain parameters to vary between modalities. In addition, multiple strain imaging techniques may be available in clinical practice, and the clinician should decide which technique to use. Therefore, this study aims to compare predictive performance of different strain parameters using multiple imaging techniques, in relation to CRT response.

Methods

Study population

This pre-defined sub-study with focus on myocardial strain imaging techniques is part of the Markers and Response to CRT (MARC) study, designed to investigate predictors of CRT response. The MARC study included 240 patients planned for CRT implantation in six medical centres in the Netherlands. Details on the original MARC study were published previously.[17] In this sub-study, 27 patients were included to undergo a comprehensive imaging protocol including CMR myocardial tagging. Because the dedicated CMR-TAG algorithm was only available in VU University Medical Center (Amsterdam, The Netherlands), patients included at this site and two nearby centres being Academic Medical Center (Amsterdam, The Netherlands) and University Medical Center Utrecht (Utrecht, The Netherlands) gave consent for additional CMR examination at VU University Medical Center. All patients gave written informed consent, and all local medical ethics committees approved data collection and

management. The investigation conforms to the principles outlined in the Declaration of Helsinki.

Image acquisition: cardiovascular magnetic resonance imaging

All patients underwent CMR examination at the VU University Medical Center (Amsterdam, The Netherlands) on a 1.5T whole body system (Magnetom Avanto, Siemens, Erlangen, Germany) with the use of a phased array cardiac receiver coil. Both CMR cine images for CMR-FT analysis and CMR-TAG images were obtained in the same examination. Standard CMR cine images were acquired using a retrospectively electrocardiogram-gated balanced steady-state free-precession sequence during end-expiratory breath holding. A stack of short-axis cine images was acquired covering the full LV. Subsequently, high temporal resolution cine imaging of the LV in the three-chamber view was performed to assess the opening and closure times of the mitral and aortic valve. Tagged images were acquired at the basal and mid-LV short-axis slices using a complementary spatial modulation of magnetization line tagging sequence with segmented electrocardiogram-gated acquisitions and serial breath holds.[18] Typical image acquisition parameters are reported in the Supporting Information.

Image acquisition: echocardiography

Echocardiographic examinations were performed by participating centres and sent to the echocardiographic core lab (University Medical Center Utrecht, Utrecht, The Netherlands) for detailed analysis. Examinations were performed on GE Vivid7, GE Vivid9, or Philips iE33 ultrasound machines. Standard echocardiographic images were obtained, including a parasternal short-axis (PSAX) view at the papillary muscle level and at the mitral valve level and an apical four-chamber (AP4CH) view, zoomed, and focused on the LV. An additional zoomed and trimmed image of the interventricular septum in the AP4CH was recorded for septal single wall analysis with higher frame rates. Images were obtained at three consecutive beats. Image quality and frame rate of all images were optimized for offline speckle tracking analysis. Pulsed-wave Doppler images of the LV outflow tract and mitral valve inlet were obtained for definition of aortic valve and mitral valve closure, respectively.

Image post-processing

Strain analysis was performed in the circumferential (CMR-TAG, CMR-FT, and STE-circ) and longitudinal (STE-long) orientations. Post-processing of CMR-TAG images was performed

by dedicated software using the SinMod technique (*inTag* v2.0, CREATIS, Lyon, France),[19] as a plug-in for OsiriX (v6.5, Pixmeo, Switzerland). Semi-automated CMR-FT analysis software (*QStrain Research Edition* v1.3.0.10 evaluation version, Medis, Leiden, The Netherlands) was used to analyse short-axis cine images corresponding with the mid-LV and basal slice location of the CMR-TAG images. Echocardiographic images of the two PSAX views (STE-circ), AP4CH view, and septal single wall (STE-long) were used for offline speckle tracking analysis. Images were exported as DICOM files for vendor independent strain analysis with TomTec 2D Cardiac Performance Analysis (v1.2.1.2, TomTec Imaging Systems GmbH, Munich, Germany). A detailed description of the post-processing steps for the CMR-TAG, CMR-FT, and STE analyses has been published previously and is given in the Supporting Information.[20]

Strain parameters

Five subsets of strain parameters were evaluated. Firstly, basic strain values were quantified by the septal and lateral peak negative strain (peak strain) and end-systolic strain (ESS) at aortic valve closure. Secondly, dyssynchrony was measured as septal to lateral delay in onset shortening (onset-delay), peak contraction (peak-delay),[21] and the standard deviation in time to peak of the total LV (SD-TTP$_{LV}$).[22] Thirdly, discoordination of the septal and lateral wall was measured by systolic rebound stretch of the septum (SRS$_{sep}$),[7] systolic stretch index (SSI$_{sep-lat}$),[9] and the internal stretch index (ISF$_{sep-lat}$). Fourthly, discoordination parameters that include all LV segments were calculated by the circumferential uniformity ratio estimate (CURE$_{LV}$) index[13] and the internal stretch index of the total LV (ISF$_{LV}$).[8] Lastly, septal strain patterns were visually categorized to the following pre-specified septal strain patterns: double peaked systolic shortening (LBBB-1); early pre-ejection shortening followed by prominent systolic stretch (LBBB-2); or pseudo-normal shortening with a late-systolic shortening peak and less pronounced end-systolic stretch (LBBB-3).[23] Strain parameters are illustrated in *Figure 1* and further explained in the Supporting Information.

Assessment of cardiac resynchronization therapy response

Echocardiographic assessment of LV volumes was performed before and 12 months after CRT implantation. Left ventricular end-systolic volume (LVESV) was measured using the biplane Simpson's method by two experienced observers. Volumetric response was calculated as the per cent change in LVESV between baseline and 12 months' follow-up. Patients with ≥15% reduction in LVESV were classified as CRT responders.

Statistical analysis

Statistical analysis was performed in the study core lab (University Medical Center Groningen, Groningen, The Netherlands) by B. G. and M. R. using the commercially available R software (R Foundation for Statistical Computing, Vienna, Austria). Continuous variables are expressed as mean ± standard deviation or in absence of a normal distribution as median and interquartile range. Categorical variables are presented as absolute numbers and percentages. Strain parameters were compared between CRT responder groups by an independent Student's *t*-test or a non-parametric test when appropriate. Correlations between strain parameters and volumetric CRT response were assessed using the Pearson's correlation coefficient or when normal distribution was absent, the Spearman's rho correlation coefficient. Receiver operating characteristic curve analysis was used to determine the predictive value of all parameters. To test the additional value of strain parameters on top of guideline criteria, multivariable linear regression analysis was performed by addition of the best performing strain parameter (based on R^2) to a model with QRS duration and QRS morphology. A *P*-value of <0.05 was considered statistically significant.
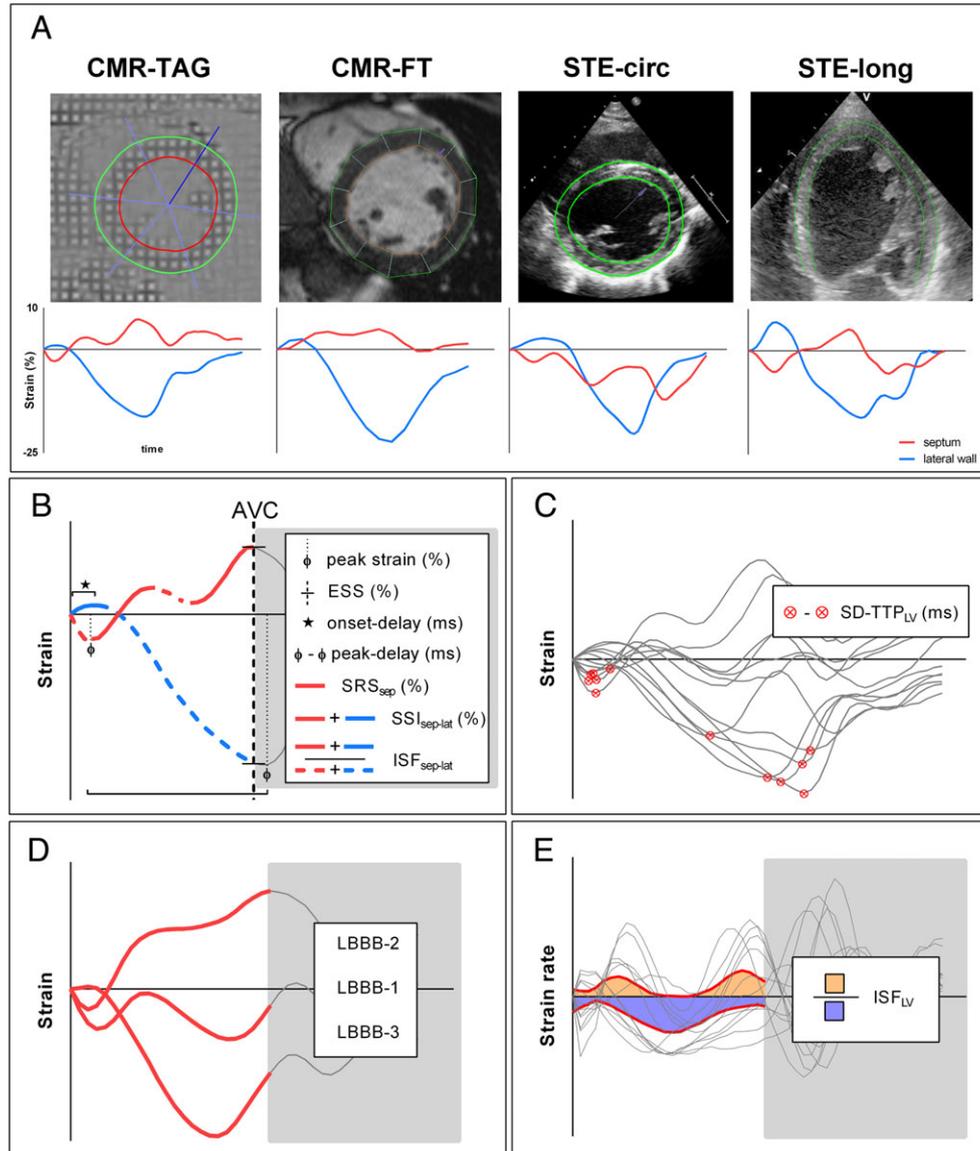
Results

Twenty-six patients completed the study protocol including clinical follow-up of 12 months. One patient was lost to follow-up because of non-cardiac death (lung carcinoma). A detailed description of the patient characteristics is given in *Table 1*. Mean LVESV change after 12 months was −29 ± 27% with 17 (65%) patients becoming CRT responders.

Strain parameters and their relation to cardiac resynchronization therapy response

Basic strain values measured as peak strain of the septal and lateral wall showed weak correlations with LVESV change as demonstrated in *Figure 2*. On the other hand, ESS$_{sep}$ showed one of the highest coefficients of determination of all parameters using CMR-TAG (R^2 0.60; $P < 0.001$). Other imaging techniques showed good results for ESS$_{sep}$ as well (CMR-FT R^2 0.50, STE-circ R^2 0.43, and STE-long R^2 0.43) as illustrated in *Figure 3*. Dyssynchrony of all LV segments measured by SD-TTP$_{LV}$ showed high correlations using CMR-TAG (R^2 0.61; $P < 0.001$), but was disappointing for other imaging techniques (all $R^2 \leq 0.14$). Other dyssynchrony measures (onset-delay and peak-delay) showed weaker coefficients of determination with LVESV change, and results were subject to large variation between imaging techniques. Discoordination

Figure 1 Imaging techniques and strain parameters. (A) Typical example of a left bundle branch block (LBBB) patient with strain analysis in the circumferential [cardiovascular magnetic resonance (CMR) tagging (CMR-TAG), CMR feature tracking (CMR-FT), and speckle tracking echocardiography (STE)-circ] and longitudinal (STE-long) orientations. (B) Strain parameters calculated from the septal (red) and/or lateral (blue) wall including peak negative peak strain (peak strain), end-systolic strain (ESS), septal to lateral time delay onset contraction (onset-delay) and delay in peak contraction (peak-delay), systolic rebound stretch of the septum (SRS_{sep}), systolic stretch index ($SSI_{sep-lat}$), and internal stretch index ($ISF_{sep-lat}$). (C) The standard deviation of time to peak strain of all segments ($SD-TTP_{LV}$). (D) Septal strain patterns defined as double peaked shortening (LBBB-1); predominant stretching (LBBB-2); or pseudo-normal shortening (LBBB-3). (E) The internal stretch factor including all left ventricular (LV) segments (ISF_{LV}).

markers measured from the septal and lateral wall were all moderately associated with LVESV change, and predictive performance was similar for different imaging techniques. Of these parameters, $ISF_{sep-lat}$ showed best results (CMR-TAG R^2 0.47, CMR-FT R^2 0.39, STE-circ R^2 0.48, and STE-long R^2 0.39; all $P < 0.001$). Discoordination of all LV segments measured by ISF_{LV} yielded one of the highest coefficients of determination using CMR-TAG (R^2 0.57; $P < 0.001$) while other imaging techniques showed poor results (all $R^2 \leq 0.32$). The

$CURE_{LV}$ parameter showed weak coefficients of determination with LVESV change, irrespective of imaging technique.

Visual classification of septal strain patterns

As demonstrated in *Figure 4*, CMR-TAG and CMR-FT classified half of the patients as LBBB-2 pattern, whereas LBBB-2 pattern was found in only a quarter of the patients by means of STE

Table 1 Patient characteristics at baseline and at 12 months' follow-up

Variable	Total group (n = 26)	Responders (n = 17)	Non-responders (n = 9)
Age (years)	65 ± 9	63 ± 10	68 ± 8
Gender (*n*, % male)	15 (58%)	9 (53%)	6 (67%)
QRS duration (ms)	182 (166–193)	187 (180–202)**	165 (143–176)**
QRS morphology	21 (81%)	16 (94%)*	5 (56%)*
(*n*, % LBBB)			
Aetiology (*n*, % ICMP)	7 (27%)	1 (6%)**	6 (67%)**
NYHA class (*n*, %)			
II	17 (65%)	12 (71%)	5 (56%)
III	9 (35%)	5 (29%)	4 (44%)
Medication (*n*, %)			
Beta-blockers	22 (85%)	15 (88%)	7 (78%)
Diuretics	21 (81%)	14 (83%)	7 (78%)
ACE/ATII inhibitors	17 (65%)	11 (65%)	6 (67%)
Aldosterone antagonist	10 (38%)	8 (47%)	2 (22%)
Lab			
Creatinine value (unit)	76 (68–85)	76 (67–79)	80 (69–95)
BNP value (unit)	636 (230–1603)	686 (276–1591)	554 (214–1607)
CMR			
LVEDV (mL)	313 ± 100	348 ± 105**	248 ± 46**
LVESV (mL)	234 ± 98	266 ± 105**	174 ± 44**
LVEF (%)	27 ± 9	25 ± 10	30 ± 6
LV mass (g)	130 (117–156)	145 (124–173)*	115 (97–132)*
Scar (% LV mass)	1.8 (0.0–8.6)	0.0 (0.0–1.9)**	9.4 (5.0–19.5)**
Scar pattern (*n*, % ICMP)	8 (31%)	2 (12%)**	6 (67%)**
RVEF (%)	51 ± 12	49 ± 13	54 ± 10
Echo			
Change in LVESV after 12 months (%)	−29 ± 27	−44 ± 17**	0 ± 14**

ACE/ATII, angiotensin-converting enzyme/angiotensin II; BNP, brain natriuretic peptide; CMR, cardiovascular magnetic resonance; ICMP, ischaemic cardiomyopathy; LBBB, left bundle branch block; LV, left ventricular; LVEDV, left ventricular end-diastolic volume; LVEF, left ventricular ejection fraction; LVESV, left ventricular end-systolic volume; NYHA, New York Heart Association; RVEF, right ventricular ejection fraction.
*Statistical difference between responders and non-responders marked with $P < 0.05$.
**Statistical difference between responders and non-responders marked with $P < 0.01$.

techniques. In general, the LBBB-2 pattern was associated with the largest reduction in LVESV, irrespective of its technique. Patients with pattern LBBB-1 showed less reverse remodelling, and results differed more between techniques. The LBBB-3 pattern is in particular of interest to exclude non-responders to CRT, but only CMR-TAG was accurate in doing this.

Patient characteristics and their role in cardiac resynchronization therapy response

In this study, patients with ischaemic cardiomyopathy (ICMP) showed less reduction in LVESV compared with patients with non-ICMP (−7 ± 30% vs. −36 ± 21%; $P = 0.010$). In addition, scar size was significantly related with LVESV change ($R^2 = 0.42$; $P < 0.001$). Subgroup analysis by gender revealed no significant differences in LVESV change between men and women (−24 ± 27% vs. −35 ± 26%; $P = 0.295$). Patients with QRS duration ≥150 ms showed a trend towards more LVESV change compared with <150 ms patients (−33 ± 24% vs. −6 ± 33%; $P = 0.063$). However, patients with strict LBBB morphology showed a significantly larger LVESV reduction compared with patients with intraventricular conduction delay morphology (−35 ± 24% vs. −3 ± 22%; $P = 0.013$).

Septal strain in relation to present guideline criteria

QRS duration and QRS morphology were both significantly related with CRT response in univariable linear regression analysis. Subsequently, the best overall performing strain parameter by means of the highest R^2 in relation to LVESV change, ESS_{sep}, was implemented in a multivariable model. Multivariable linear regression analysis showed that ESS_{sep} remained independently related to LVESV change after adjustment for QRS duration and QRS morphology as demonstrated in *Table 2*. This finding was irrespective of the imaging technique used for ESS_{sep} assessment (adjusted models 1–4).

Discussion

This study offered the unique opportunity to compare a variety of strain parameters using multiple imaging techniques in a population that is eligible for CRT. Measures of dyssynchrony (SD-TTP$_{LV}$) and discoordination (ISF$_{LV}$) were strongly related to CRT response when using CMR-TAG. However, these parameters showed weaker correlations for CMR-FT and STE techniques. In contrast, the end-systolic septal

Figure 2 Coefficient of determination (R^2) of all strain parameters towards reverse remodelling after cardiac resynchronization therapy. Coefficient of determination of all strain parameters towards changes in LVESV after 12 months' cardiac resynchronization therapy is displayed for CMR-TAG (red), CMR-FT (blue), STE-circ (green), and STE-long (orange). For other abbreviations, see *Figure 1*.
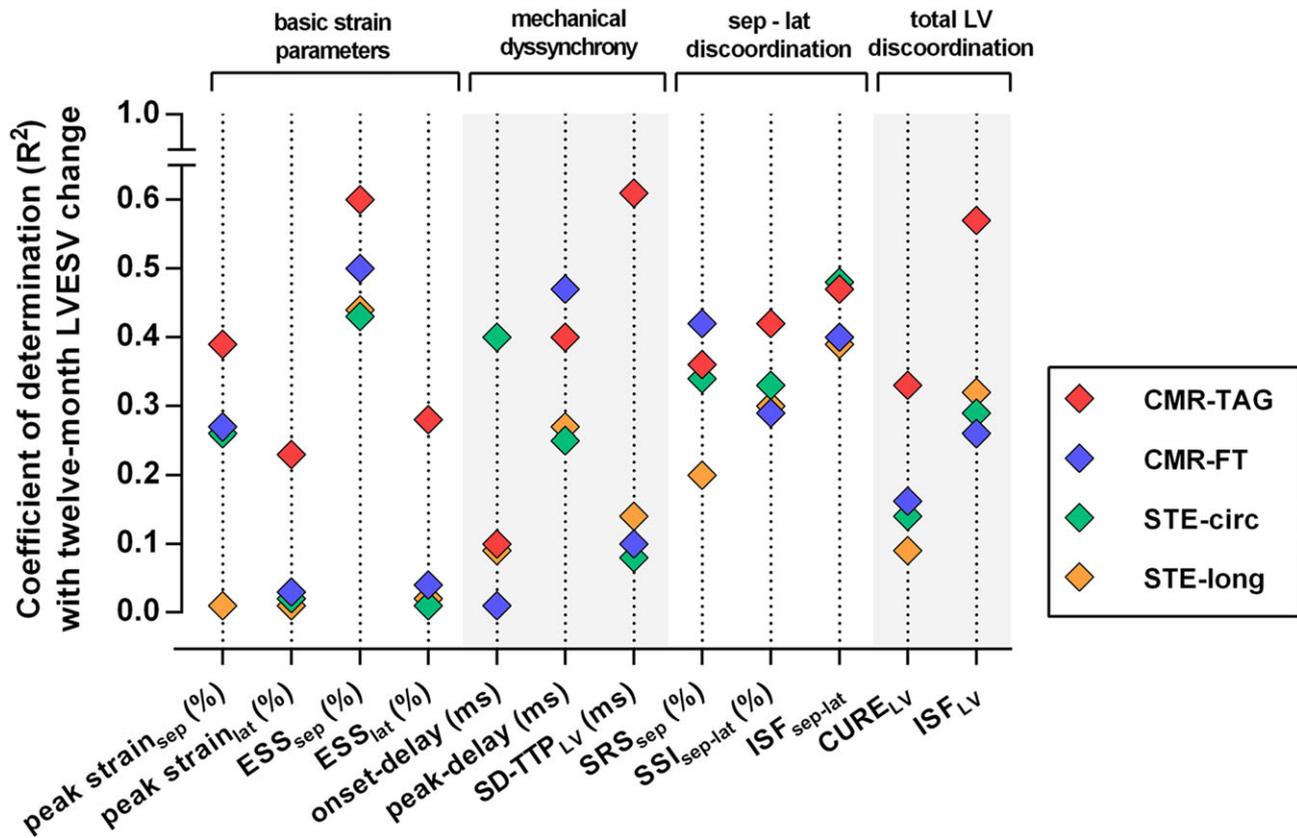
strain parameter showed a consistent good relation to reverse remodelling after CRT, irrespective of assessment technique. This parameter demonstrated predictive value on top of current guideline criteria for each imaging technique.

Comparison of strain parameters

Two types of strain parameters that can be assessed are dyssynchrony (regional timing differences in time units) and discoordination (inefficient contraction patterns in percentage strain units). Both types can be calculated on a regional (i.e. septal to lateral) and segmental (i.e. 17 segments model) scale. In patients with LBBB, dyssynchrony is a direct consequence of the conduction disorder with early activation of the septum and delayed activation of the lateral wall. Contraction of the septum takes place under low LV pressure (i.e. low wall tension) whereas the lateral wall contracts during rising LV pressures, thus increasing regional workload.[4] Consequently, compensatory mechanisms increase contractility of the lateral wall whereas contractility of the septum is reduced. This results in the lateral wall pushing the septum back during systole (i.e. discoordination), reducing LV pump

function efficiency. Our results indicate that both dyssynchrony and discoordination parameters measured on a segmental scale (i.e. SD-TTP$_{LV}$ and ISF$_{LV}$) were strongly related with CRT response. These measures use 12 individual segments distributed over the basal and mid-LV slice to quantify the total amount of mechanical substrate for resynchronization. From a physiological point of view, the ISF$_{LV}$ parameter proposed by Kirn *et al*. is closest related to the amount of inefficient pump function that can be attributed to the LBBB conduction disorder by indexing the amount of systolic stretching (i.e. wasting myocardial work) to the amount of systolic shortening (i.e. useful myocardial work).[8] In contrast, assessing the circumferential uniformity of segmental strain values by complex Fourier analysis (i.e. CURE index) showed rather disappointing association with CRT response.[13] Possibly, the presence of stretching segments instead of non-uniformity in contraction determines benefit from CRT.

Septal strain analysis

Typical septal contraction patterns have been described to identify 'true' LBBB activation using patient data combined

Figure 3 Correlation between end-systolic septal strain (ESS$_{sep}$) and left ventricular end-systolic volume (LVESV) change per imaging technique. The basic strain parameter ESS$_{sep}$ consistently shows a high coefficient of determination with LVESV change independent of imaging modality: (A) cardiovascular magnetic resonance (CMR) tagging (CMR-TAG), (B) feature tracking (CMR-FT), (C) speckle tracking echocardiography (STE)-circ, and (D) STE-long.
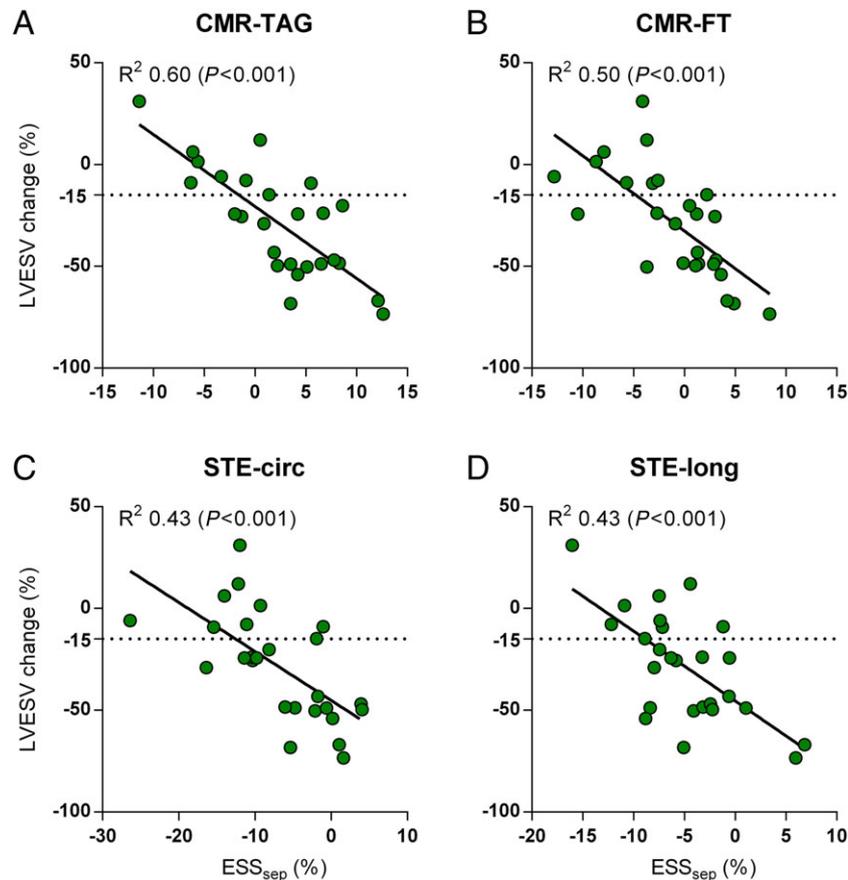
with computer modelling.[16,24,25] Typical LBBB strain patterns were characterized by double peaked shortening (LBBB-1) or predominant stretching (LBBB-2) of the septum.[23] Patients lacking true LBBB activation were characterized by pseudo-normal shortening of the septum (LBBB-3) and showed less reverse remodelling compared with LBBB-1 and LBBB-2 patients. Quantification of septal behaviour by end-systolic septal strain (ESS$_{sep}$) showed a consistent high correlation with LVESV change, irrespective of imaging technique (*Figure 3*). Of note, ESS$_{sep}$ and the septal strain patterns are interdependent as a negative ESS$_{sep}$ value represents LBBB-3 pattern whereas positive ESS$_{sep}$ values represent LBBB-2 pattern. Assessment of ESS$_{sep}$ is relatively simple as illustrated in *Figure 1* and requires strain analysis of the septum only. We found more positive ESS$_{sep}$ values (i.e. net septal stretch throughout systole) to be associated with more extensive reverse remodelling after CRT. Preserved septal contraction by a negative ESS$_{sep}$, on the other hand, showed less room for improvement after CRT. Previous studies showed that electrical resynchronization improves systolic function by recruiting myocardial work from

the septum.[6,7] Therefore, SRS$_{sep}$ is used to predict CRT outcome.[7,9,26] In our study, ESS$_{sep}$ was even closer related with LVESV changes than SRS$_{sep}$, possibly because ESS$_{sep}$ is the result of both systolic shortening and stretching whereas SRS$_{sep}$ merely measures the cumulative amount of systolic stretching. In a multivariable model, ESS$_{sep}$ demonstrated predictive value on top of guideline criteria (i.e. QRS duration and QRS morphology) irrespective of the imaging technique used.

Comparison of strain imaging techniques

Previously, we compared strain values between imaging techniques and found that most parameters were not interchangeable for different modalities.[20] The present study demonstrates that there is only one parameter that performs equally well for all techniques, when related to CRT response. For the other strain parameters, CMR-TAG demonstrated higher correlation coefficients with LVESV change compared with other imaging techniques. Strain parameters including

Figure 4 Classification of septal strain patterns to estimate cardiac resynchronization therapy response. Septal strain patterns are classified to pre-specified categories: double peaked shortening (LBBB-1); predominant stretching (LBBB-2); or pseudo-normal shortening (LBBB-3) using (A) cardiovascular magnetic resonance (CMR) tagging (CMR-TAG), (B) feature tracking (CMR-FT), (C) speckle tracking echocardiography (STE)-circ, and (D) STE-long. Statistical differences between septal strain patterns are marked with an asterisk.
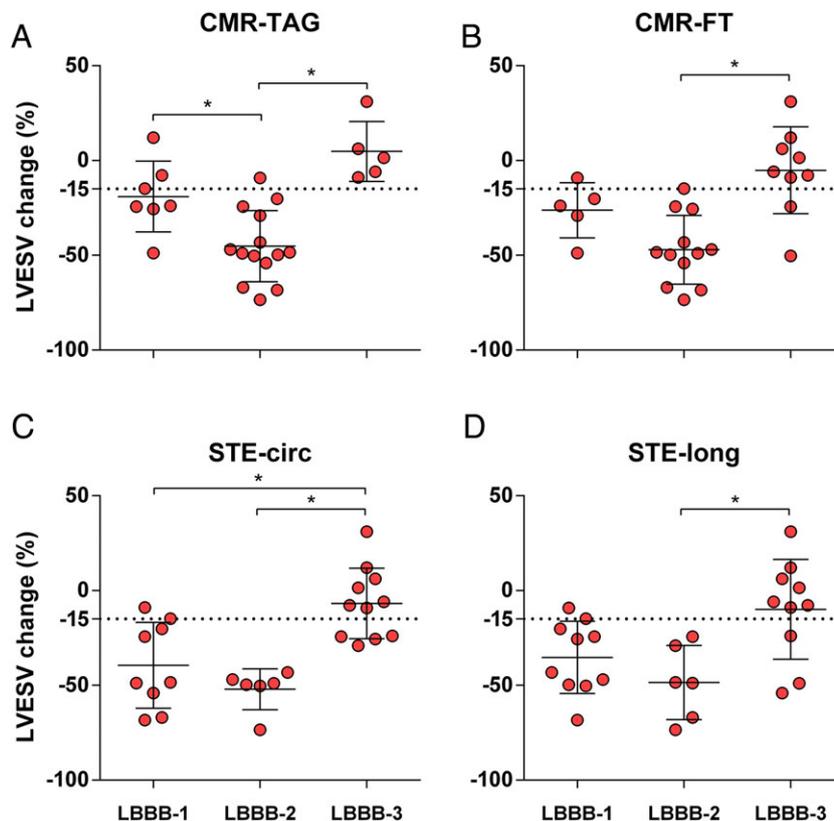

Table 2 Linear regression analysis to test the additional value of end-systolic septal strain on top of guideline criteria per imaging technique

Guideline criteria + ESS$_{sep}$ per imaging technique	Univariable analysis			Adjusted Model 1		
CMR tagging	Beta	95% CI	P-value	Beta	95% CI	P-value
QRS duration (per ms)	−0.41	−0.74 to −0.09	0.015	−0.18	−0.42 to 0.07	0.146
QRS morphology (LBBB)	−31.99	−56.45 to −7.53	0.013	−10.63	−29.55 to 8.29	0.256
CMR-TAG ESS$_{sep}$ (per %)	−3.54	−4.77 to −2.32	<0.001	−2.95	−4.25 to −1.66	<0.001
CMR feature tracking				Adjusted Model 2		
QRS duration (per ms)	−0.41	−0.74 to −0.09	0.015	−0.15	−0.42 to 0.12	0.265
QRS morphology (LBBB)	−31.99	−56.45 to −7.53	0.013	−17.68	−37.52 to 2.17	0.078
CMR-FT ESS$_{sep}$ (per %)	−3.69	−5.26 to −2.13	<0.001	−2.99	−4.56 to −1.42	0.001
STE circumferential				Adjusted Model 3		
QRS duration (per ms)	−0.41	−0.74 to −0.09	0.015	−0.20	−0.49 to 0.09	0.172
QRS morphology (LBBB)	−31.99	−56.45 to −7.53	0.013	−13.27	−36.13 to 9.60	0.242
STE-circ ESS$_{sep}$ (per %)	−2.41	−3.59 to −1.23	<0.001	−1.81	−3.08 to −0.54	0.007
STE longitudinal				Adjusted Model 4		
QRS duration (per ms)	−0.41	−0.74 to −0.09	0.015	−0.20	−0.51 to 0.10	0.186
QRS morphology (LBBB)	−31.99	−56.45 to −7.53	0.013	−7.31	−33.20 to 18.58	0.564
STE-circ ESS$_{sep}$ (per %)	−3.43	−5.08 to −1.79	<0.001	−2.62	−4.70 to −0.54	0.016

CI, confidence interval; CMR, cardiovascular magnetic resonance; CMR-FT, CMR feature tracking; CMR-TAG, CMR tagging; ESS$_{sep}$, end-systolic septal strain; LBBB, left bundle branch block; STE, speckle tracking echocardiography.

all LV segments (i.e. ISF_{LV} and $SD\text{-}TTP_{LV}$) performed best for CMR-TAG, but results were rather disappointing for CMR-FT and STE techniques. Differences were most pronounced for $SD\text{-}TTP_{LV}$ measuring the standard deviation in segmental time to peak contraction throughout the LV. A possible explanation for this finding might be that measuring $SD\text{-}TTP_{LV}$ requires not only high image quality to visualize all individual segments, but also sufficient temporal resolution to measure segmental timing differences. CMR-TAG combines excellent image quality with high frame rates whereas CMR-FT might be hampered by the lower temporal resolution that was used for cine imaging and STE by the lower image quality and higher inter-study variation compared with CMR-TAG.[27] In this study, temporal resolution of the cine images for CMR-FT analysis was lower compared with the high temporal resolution of the CMR-TAG sequence (~40 vs. ~14 ms). Using higher temporal resolutions for CMR-FT might improve predictive performance of this technique, although a temporal resolution of ~40 ms is typically used in standard cine-imaging protocols. CMR-FT enables myocardial strain analysis using specialized post-processing software on standard cine images.[12,28] Although this relatively new technique has not been extensively validated yet, we recently showed reasonable agreement with CMR-TAG.[20] Predictive performance of CMR-FT was highest for strain parameters derived from the septal and lateral wall (ESS_{sep}, peak-delay, SRS_{sep}, and $ISF_{sep-lat}$) whereas parameters including all LV segments ($SD\text{-}TTP_{LV}$ and ISF_{LV}) were poorly related to CRT response. Possibly, the measurement variability of CMR-FT is too high to sample strain on a segmental scale.[29] Despite promising results of septal strain measures in the present study, data on CMR-FT in this specific patient population are scarce and further validation of this technique is needed.

In general, performance of STE was comparable with CMR-FT. Speckle tracking echocardiography analysis was performed in both the circumferential and longitudinal directions, each with associated strengths and weaknesses. Circumferential strain markers are considered to be more sensitive to deformation abnormalities because of the predominant circumferential fibre orientation.[30] Echocardiographic image quality, however, is often more favourable in the AP4CH view (STE-long) compared with the PSAX view (STE-circ). Taken together, overall performance of STE-circ and STE-long was very similar.

Clinical implications

Myocardial strain imaging provides new diagnostic tools that could potentially improve patient selection for CRT. At present, various strain parameters and multiple imaging techniques have been proposed to serve as clinical markers of CRT response. In a first step to evaluate the clinical implications of these markers, we performed a systematic comparison of strain parameters on a multi-modality level. We found the end-systolic septal strain parameter to be strongly related to CRT response, irrespective of modality. Although CMR-TAG demonstrates overall superior results compared with other imaging techniques, its availability is limited in clinical practice. On the other hand, standard CMR imaging is increasingly used to screen CRT candidates by measuring LV ejection fraction combined with scar visualization to target LV lead placement.[31] Additional CMR-FT strain analysis of the septum could potentially expand diagnostic yield of this comprehensive imaging technique. When CMR imaging is not accessible, STE can also be used as a good alternative to estimate CRT benefit. In general, the end-systolic septal strain parameter can be obtained by any available strain imaging technique and provides predictive value on top of current guideline criteria. The application of strain imaging has yet not been included in daily practice, but it is likely to become a useful application when evaluating heart failure patients for CRT implantation. This may be of particular interest in CRT candidates with unfavourable patient characteristics (ICMP, intraventricular conduction delay morphology, and shorter QRS duration), in whom benefit from CRT is doubted.

Limitations

The relatively small sample size is the main limitation of this study. Because of the limited availability of CMR-TAG sequences and post-processing software in clinical practice, only a small proportion of the original MARC population was included in the present sub-study. Despite the limited sample size, this is the first study to perform a systematic comparison between strain parameters and strain imaging techniques in relation to CRT response. Secondly, only a small proportion of the patients had ICMP, which limits the confounding effects of scar tissue on strain parameters. For example, a myocardial infarction located at the septum might influence septal strain assessment with less negative or even positive strain values due to akinetic tissue or passive stretching, thus resembling strain patterns seen in patients with explicit discoordination. Unfortunately, the number of patients with myocardial infarction was too low to evaluate the effects of septal scar on strain parameters. The influence of scarred segments, however, has previously been investigated for other discoordination parameters. These studies showed a limited effect of myocardial scarring on the predictive value of these parameters.[7,9,23]

Conclusions

In conclusion, end-systolic septal strain showed a consistent good relation to reverse remodelling after CRT, irrespective of the technique used for assessment. Measuring end-

systolic septal strain by any available strain imaging technique provides predictive value on top of current guideline criteria.

Conflict of interest

Funding

Supporting information

Additional supporting information may be found online in the Supporting Information section at the end of the article.

Figure S1. Correlation between conventional strain markers quantified by the CMR-TAG technique and LVESV change.
Figure S2. Correlation between the internal stretch factor of the septal and lateral wall (ISF$_{sep-lat}$) and LVESV change per imaging technique.
Table S1. Comparison of strain parameters between responders (R) and non-responders (NR).
Table S2. Coefficient of determination (R^2) and area under the curve (AUC) of strain parameters and CRT response (echocardiographic LVESV change after 12 months).
Table S3. Predictive value of strain parameters for CRT volumetric response (reduction in LVESV at 12 months ≥15%).
Table S4. Septal strain patterns and volumetric CRT response (echocardiographic LVESV change after 12 months).
Table S5. Predictive value of septal strain patterns for volumetric CRT response (reduction in LVESV at 12 months ≥15%).

References

1. Ponikowski P, Voors AA, Anker SD, Bueno H, Cleland JG, Coats AJ, Falk V, Gonzalez-Juanatey JR, Harjola VP, Jankowska EA, Jessup M, Linde C, Nihoyannopoulos P, Parissis JT, Pieske B, Riley JP, Rosano GM, Ruilope LM, Ruschitzka F, Rutten FH, van der Meer P. ESC guidelines for the diagnosis and treatment of acute and chronic heart failure: the Task Force for the diagnosis and treatment of acute and chronic heart failure of the European Society of Cardiology (ESC) developed with the special contribution of the Heart Failure Association (HFA) of the ESC. *Eur Heart J* 2016; **37**: 2129–2200.

2. Daubert C, Behar N, Martins RP, Mabo P, Leclercq C. Avoiding non-responders to cardiac resynchronization therapy: a practical guide. *Eur Heart J* 2016; ehw270.

3. Khidir MJ, Delgado V, Ajmone Marsan N, Schalij MJ, Bax JJ. QRS duration versus morphology and survival after cardiac resynchronization therapy. *ESC Heart Fail* 2017; **4**: 23–30.

4. Zweerink A, de Roest GJ, Wu L, Nijveldt R, de Cock CC, van Rossum AC, Allaart CP. Prediction of acute response to cardiac resynchronization therapy by means of the misbalance in regional left ventricular myocardial work. *J Card Fail* 2016; **22**: 133–142.

5. Prinzen FW, Vernooy K, De Boeck BW, Delhaas T. Mechano-energetics of the asynchronous and resynchronized heart. *Heart Fail Rev* 2011; **16**: 215–224.

6. Russell K, Eriksen M, Aaberge L, Wilhelmsen N, Skulstad H, Gjesdal O, Edvardsen T, Smiseth OA. Assessment of wasted myocardial work: a novel method to quantify energy loss due to uncoordinated left ventricular contractions. *Am J Physiol Heart Circ Physiol* 2013; **305**: H996–H1003.

7. De Boeck BWL, Teske AJ, Meine M, Leenders GE, Cramer MJ, Prinzen FW, Doevendans PA. Septal rebound stretch reflects the functional substrate to cardiac resynchronization therapy and predicts volumetric and neurohormonal response. *Eur J Heart Fail* 2009; **11**: 863–871.

8. Kirn B, Jansen A, Bracke F, van Gelder B, Arts T, Prinzen FW. Mechanical discoordination rather than dyssynchrony predicts reverse remodeling upon cardiac resynchronization. *Amer J Physiol-Heart Circul Physiol* 2008; **295**: H640–H646.

9. Lumens J, Tayal B, Walmsley J, Delgado-Montero A, Huntjens PR, Schwartzman D, Althouse AD, Delhaas T, Prinzen FW, Gorcsan J III. Differentiating electromechanical from non-electrical substrates of mechanical discoordination to identify responders to cardiac resynchronization

therapy. *Circ Cardiovasc Imaging* 2015; **8**: e003744.

10. Jackson T, Sohal M, Chen Z, Child N, Sammut E, Behar J, Claridge S, Carr-White G, Razavi R, Rinaldi CA. A U-shaped type II contraction pattern in patients with strict left bundle branch block predicts super-response to cardiac resynchronization therapy. *Heart Rhythm* 2014; **11**: 1790–1797.

11. Revah G, Wu V, Huntjens PR, Piekarski E, Chyou JY, Axel L. Cardiovascular magnetic resonance features of mechanical dyssynchrony in patients with left bundle branch block. *Int J Cardiovasc Imaging* 2016; **32**: 1427–1438.

12. Pedrizzetti G, Claus P, Kilner PJ, Nagel E. Principles of cardiovascular magnetic resonance feature tracking and echocardiographic speckle tracking for informed clinical use. *J Cardiovasc Magn Reson* 2016; **18**: 51.

13. Bilchick KC, Dimaano V, Wu KC, Helm RH, Weiss RG, Lima JA, Berger RD, Tomaselli GF, Bluemke DA, Halperin HR, Abraham T, Kass DA, Lardo AC. Cardiac magnetic resonance assessment of dyssynchrony and myocardial scar predicts function class improvement following cardiac resynchronization therapy. *J Am Coll Cardiol Img* 2008; **1**: 561–568.

14. Russel IK, Zwanenburg JJ, Germans T, Marcus JT, Allaart CP, de Cock CC, Gotte

MJ, van Rossum AC. Mechanical dyssynchrony or myocardial shortening as MRI predictor of response to biventricular pacing? *J Magn Reson Imaging* 2007; **26**: 1452–1460.

15. Andersson LG, Wu KC, Wieslander B, Loring Z, Frank TF, Maynard C, Gerstenblith G, Tomaselli GF, Weiss RG, Wagner GS, Ugander M, Strauss DG. Left ventricular mechanical dyssynchrony by cardiac magnetic resonance is greater in patients with strict vs nonstrict electrocardiogram criteria for left bundle-branch block. *Am Heart J* 2013; **165**: 956–963.

16. Risum N, Tayal B, Hansen TF, Bruun NE, Jensen MT, Lauridsen TK, Saba S, Kisslo J, Gorcsan J III, Sogaard P. Identification of typical left bundle branch block contraction by strain echocardiography is additive to electrocardiography in prediction of long-term outcome after cardiac resynchronization therapy. *J Am Coll Cardiol.* 2015; **66**: 631–641.

17. Maass AH, Vernooy K, Wijers SC, van 't Sant J, Cramer MJ, Meine M, Allaart CP, De Lange FJ, Prinzen FW, Gerritse B, Erdtsieck E, Scheerder COS, Hill MRS, Scholten M, Kloosterman M, Ter Horst IAH, Voors AA, Vos MA, Rienstra M, Van Gelder IC. Refining success of cardiac resynchronization therapy using a simple score predicting the amount of reverse ventricular remodelling: results from the Markers and Response to CRT (MARC) study. *Europace* 2018; **20**: e1-e10.

18. Zwanenburg JJ, Gotte MJ, Kuijer JP, Heethaar RM, van Rossum AC, Marcus JT. Timing of cardiac contraction in humans mapped by high-temporal-resolution MRI tagging: early onset and late peak of shortening in lateral wall. *Am J Physiol Heart Circ Physiol* 2004; **286**: H1872–H1880.

19. Miller CA, Borg A, Clark D, Steadman CD, McCann GP, Clarysse P, Croisille P, Schmitt M. Comparison of local sine wave modeling with harmonic phase analysis for the assessment of myocardial strain. *J Magn Reson Imaging* 2013; **38**: 320–328.

20. van Everdingen WM, Zweerink A, Nijveldt R, Salden OAE, Meine M, Maass AH, Vernooy K, De Lange FJ, van Rossum AC, Croisille P, Clarysse P, Geelhoed B, Rienstra M, Van Gelder IC, Vos MA, Allaart CP, Cramer MJ. Comparison of strain imaging techniques in CRT candidates: CMR tagging, CMR feature tracking and speckle tracking echocardiography. *Int J Cardiovasc Imaging* 2017; **34**: 443–456.

21. Tanaka H, Nesser HJ, Buck T, Oyenuga O, Janosi RA, Winter S, Saba S, Gorcsan J 3rd. Dyssynchrony by speckle-tracking echocardiography and response to cardiac resynchronization therapy: results of the Speckle Tracking and Resynchronization (STAR) study. *Eur Heart J* 2010; **31**: 1690–1700.

22. Pouleur AC, Knappe D, Shah AM, Uno H, Bourgoun M, Foster E, McNitt S, Hall WJ, Zareba W, Goldenberg I, Moss AJ, Pfeffer MA, Solomon SD, Investigators M-C. Relationship between improvement in left ventricular dyssynchrony and contractile function and clinical outcome with cardiac resynchronization therapy: the MADIT-CRT trial. *Eur Heart J* 2011; **32**: 1720–1729.

23. Leenders GE, Lumens J, Cramer MJ, De Boeck BW, Doevendans PA, Delhaas T, Prinzen FW. Septal deformation patterns delineate mechanical dyssynchrony and regional differences in contractility: analysis of patient data using a computer model. *Circ Heart Fail* 2012; **5**: 87–96.

24. Risum N, Strauss D, Sogaard P, Loring Z, Hansen TF, Bruun NE, Wagner G, Kisslo J. Left bundle-branch block: the relationship between electrocardiogram electrical activation and echocardiography mechanical contraction. *Am Heart J* 2013; **166**: 340–348.

25. Risum N, Jons C, Olsen NT, Fritz-Hansen T, Bruun NE, Hojgaard MV, Valeur N, Kronborg MB, Kisslo J, Sogaard P. Simple regional strain pattern analysis to predict response to cardiac resynchronization therapy: rationale, initial results, and advantages. *Am Heart J* 2012; **163**: 697–704.

26. Leenders GE, De Boeck BW, Teske AJ, Meine M, Bogaard MD, Prinzen FW, Doevendans PA, Cramer MJ. Septal rebound stretch is a strong predictor of outcome after cardiac resynchronization therapy. *J Card Fail* 2012; **18**: 404–412.

27. Grothues F, Moon JC, Bellenger NG, Smith GS, Klein HU, Pennell DJ. Interstudy reproducibility of right ventricular volumes, function, and mass with cardiovascular magnetic resonance. *Am Heart J* 2004; **147**: 218–223.

28. Schuster A, Hor KN, Kowallick JT, Beerbaum P, Kutty S. Cardiovascular magnetic resonance myocardial feature tracking: concepts and clinical applications. *Circ Cardiovasc Imaging* 2016; **9**: e004077.

29. Wu L, Germans T, Guclu A, Heymans MW, Allaart CP, van Rossum AC. Feature tracking compared with tissue tagging measurements of segmental strain by cardiovascular magnetic resonance. *J Cardiovasc Magn Reson* 2014; **2014**: 10.

30. Helm RH, Leclercq C, Faris OP, Ozturk C, McVeigh E, Lardo AC, Kass DA. Cardiac dyssynchrony analysis using circumferential versus longitudinal strain: implications for assessing cardiac resynchronization. *Circulation* 2005; **111**: 2760–2767.

31. Sommer A, Kronborg MB, Norgaard BL, Poulsen SH, Bouchelouche K, Bottcher M, Jensen HK, Jensen JM, Kristensen J, Gerdes C, Mortensen PT, Nielsen JC. Multimodality imaging-guided left ventricular lead placement in cardiac resynchronization therapy: a randomized controlled trial. *Eur J Heart Fail* 2016; **18**: 1365–1374.